Full Length

Arthritis & Rheumatism
DOI 10.1002/art.33423

Marked copy: Manuscript # ar-11-0718

Treatment of Arthritis by Macrophage Depletion and Immunomodulation: Testing an Apoptosis-Mediated Therapy in a Humanized Death Receptor Mouse Model

Jun Li, M.D., Ph.D.[1], Hui-Chen Hsu, Ph.D.[1,2], PingAr Yang, B.S. [1,2], Qi Wu, B. S. [1,2], Hao Li, M.S.[1], Laura E. Edgington, B.A. [3], Matthew Bogyo, Ph.D. [3], Robert P. Kimberly, M.D. [1], and John D. Mountz, M.D., Ph.D. [1,2]

[1] Division of Clinical Immunology and Rheumatology, Department of Medicine, University of Alabama at Birmingham, Birmingham, AL, 35294; [2] Department of Medicine, Birmingham VA Medical Center, Birmingham, AL, 35233; [3] Department of Pathology, Stanford University School of Medicine, Stanford, CA, 94305

This work was supported by a grant from Daiichi Sankyo Co., Ltd (to J.D.M.) and Lupus Research Institute (to H-C.H.). Additional support was granted from the American College of Rheumatology Research and Education Foundation for the *Within Our Reach: Finding a Cure for Rheumatoid Arthritis* campaign, the Alliance for Lupus Research – Target Identification in Lupus program, the Department of Veterans Affairs Merit Review Grant 1I01BX000600-01, the National Institutes of Health Grants 1AI 071110-01A1, ARRA 3RO1AI71110-02S1 (to J.D.M.), 1R01 EB005011-06 (to M.B.) and (1R01AI083705-01A2 to H-C.H.), and the Arthritis Investigator Award supported by the Arthritis Foundation (to H-C.H.).

Received: May 05, 2011; Revised: Sep 02, 2011; Accepted: Oct 13, 2011

Corresponding author: John D. Mountz, M.D., Ph.D.

Phone: 205-934-8909, Fax: 205-996-6788, E-mail: jdmountz@uab.edu

All authors claim to have no financial interests which could create a potential conflict of interest or the appearance of a conflict of interest with regard to the work.

Objective. To determine the therapeutic efficacy and immunomodulatory effect of an anti-human death receptor 5 (DR5) antibody, TRA-8, in eliminating macrophage subsets in a collagen II-induced arthritis (CIA) mouse model.

Methods. A chimeric human/mouse (hu/mo) DR5 transgenic (Tg) mouse, under the regulation of the mouse 3-kb promoter and a *Floxed*-STOP cassette, was generated and crossed with an ubiquitous Cre (Ubc.Cre) and a lysozyme M Cre (LysM.Cre) Tg mouse to achieve inducible- or macrophage-specific expression. CIA was induced in mice by chicken CII, which were then treated with the anti-human DR5 antibody, TRA-8. The clinical scores, histopathologic severity, macrophage apoptosis and depletion, and T cell subset development were evaluated.

Results. In hu/mo DR5 Tg Ubc.Cre mice with CIA, Tg DR5 was most highly expressed in $CD11b^+$ macrophages with lower expression on $CD4^+$ T cells. In the hu/mo DR5 Tg LysM.Cre mice, Tg DR5 was restrictively expressed in macrophages. Near infrared (NIFR) *in vivo* imaging of caspase activity and TUNEL staining demonstrated that TRA-8 rapidly induced apoptosis of macrophages in the inflammatory synovium. Depletion of pathogenic macrophages by TRA-8 leads to significantly reduced clinical scores of arthritis, decreased macrophage infiltration, synovial hyperplasia, osteoclast formation, joint destruction, cathepsin activity, inflammatory cytokine expression in joints, reduced Th17, and increased Treg cells in the draining lymph nodes (LN).

Conclusion. The anti-human DR5 antibody TRA-8 was efficacious in reducing the severity of arthritis by targeted depleting macrophages and immunomodulation. Our data provide pre-clinical evidence that TRA-8 is a potential novel biologic agent for rheumatoid arthritis (RA) therapy.

Rheumatoid arthritis (RA) is characterized by synovial hyperplasia and inflammation, with increased numbers of macrophages, fibroblasts, and lymphocytes in the synovium (1-3). Although the earliest attempts to delete $CD4^+$ T cells in the treatment of RA were disappointing (4), specific therapies to deplete B cells by anti-CD20 in RA are promising (5, 6). However, not all patients respond, and disease relapses can occur after B cell repopulation (7). Macrophages are of central importance in the pathogenesis of RA (8, 9), and disease severity correlates with the number of activated macrophages in the inflamed tissues and in circulation (10). The "professional" antigen-presenting role of macrophages has also been implicated in the pathogenesis of RA (9). Interactions between macrophages and fibroblasts, B, and T cells regulate synovial inflammation (11-13) and suggest that the macrophage is an attractive target for RA therapy. However, there has been no clinically proven efficacious and safe therapy for specific elimination of inflammatory macrophages in RA.

Human death receptor 5 (DR5) is a pro-apoptotic molecule and mediates apoptosis upon binding with its ligand, TRAIL, or an anti-DR5 agonistic antibody (14). While DR5 is found on most examined cell types, its expression is upregulated in cancer cells and it is a promising target for cancer therapy (15-17). Moreover, increased DR5 expression and susceptibility to anti-human DR5-mediated apoptosis are characteristics of the proliferating synovial fibroblasts in RA (18), though the regulation of expression and apoptotic function of DR5 in macrophages of human RA is unknown. Investigation of the therapeutic efficacy

of anti-DR5 in mouse disease models has been limited by two major obstacles. Firstly, although an antibody (MD5-1) has been developed against MK (the mouse homologue of human DR5), this antibody exhibits low cell-killing activity without a cross-linker and has not been extensively analyzed (19). Secondly, engineering a Tg mouse expressing human DR5 for testing of anti-human DR5 therapy has not been developed.

We have utilized a Tg mouse expressing a hu/mo-chimeric DR5 receptor consisting of the extracellular domain of human DR5 and the transmembrane and intracellular regions of mouse MK. This enables the binding of the anti-human DR5 antibody to the extracellular domain and the induction of apoptosis in mouse cells. Treatment with an anti-human DR5 antibody, TRA-8, successfully prevented the development of, or ameliorated the severity of, CIA when administered before or after the onset of arthritis, respectively. The major target of TRA-8 in this disease model was shown to be macrophages in which DR5 expression is upregulated. Our data provide pre-clinical evidence that the anti-human DR5 antibody, TRA-8, is a potential anti-arthritic biologic agent that preferentially eliminates macrophages and exhibits subsequent immunomodulatory effects.

MATERIALS AND METHODS

Mice. C57BL/6, UBC-*cre*/ESR1)1Ejb/J (Ubc.Cre), and B6.129-*Lyzs*$^{tm1(cre)Ifo}$/J (Lys M.Cre) mice were obtained from the Jackson Laboratory. All animal procedures were approved by The University of Alabama at Birmingham Institutional Animal Care and Use Committee.

Cell lines, cell preparation, and culture. The mouse NIH3T3 cell line was obtained from the American Type Culture Collection (ATCC, Manassas, VA) and cultured in DMEM (Invitrogen) supplemented with 10% FBS, 100 units/ml penicillin, 100 µg/ml streptomycin (Invitrogen), and 2 mM glutamine (Invitrogen) at 37ºC, 5% CO_2 in a humidified incubator. Single-cell suspensions from spleen and inguinal lymph nodes were prepared and cultured in RPMI-1640 (Invitrogen) supplemented with 10% FBS, 10 mM HEPES, and 0.1% 2-mercaptoethanol (Invitrogen).

Expression constructs, transfection, and ATPLite analysis. Human and mouse DR5 cDNAs were obtained from Open Biosystems (Huntsville, AL). The extracellular domain of human DR5 was amplified by PCR using primer **A** (huDR5For) 5'-ACTGTCGACGCCCCAAGTCAGCCTGGACACATA-3' and primer **B** (huDR5Rev) 5'-TCCTATCCAGAGGCCTAGCTTATGCCAAGAACAGGGAGAGGCAGGAGTCCCTGG-3'. Similarly, the transmembrane and intracellular domains of mouse DR5 were amplified by PCR using primer **C** (MoDR5For) 5'-

CCAGGGACTCCTGCCTCTCCCTGTTCTTGGCATAAGCTAGGCCTCTGGATA GGA-3' and primer **D** (MoDR5Rev) 5'-GATGCGGCCGCTCAAACGCACTGAGATCCTCCTGG-3'. The fused chimeric DR5 was then generated by PCR using a mixture of the A-B and C-D products as template together with primers A and D. The purified final PCR product was then digested by *Sal*I and *Not*I and this chimeric DR5 fragment was used to replace the human DR5 in the vector. A 3-kb putative mouse DR5 promoter was cloned from mouse BAC RP24-355K8 (Children's Hospital Oakland Research Institute, Oakland, CA) and subcloned upstream of the chimeric DR5. Transfection was performed using Lipofectamine 2000 (Invitrogen). Cell viability was determined using an ATP luminescence assay kit (PerkinElmer, Waltham, MA).

Establishment of the chimeric hu/mo-chim DR5 Tg mouse. The DNA used for generation of DR5 Tg mice was based the 3-kb mouse promoter/chimeric DR5 construct. To enable tissue-specific expression, a *Floxed*-STOP cassette (Addgene) was introduced between the promoter and chimeric DR5. A 8.3-kb *Drd*I-*Drd*I fragment was used to generate Tg mice on a C57BL/6 background (Transgenic Mouse Facility, UAB). The Tg mice were genotyped using the primers specific for the human DR5 extracellular domain.

Generation of hu/mo-chimeric DR5 Ubc.Cre double Tg and hu/mo-chimeric DR5 LysM.Cre double Tg mice. The *Floxed*-STOP chimeric DR5 Tg mice were

bred with two different Cre-expressing mice: (*i*) Ubc.Cre mice which have strong tamoxifen-inducible Cre activity in all tissues examined; and (*ii*) LysM.Cre mice which express Cre in myeloid cells. For Cre induction in Ubc.Cre mice, mice were treated with tamoxifen (5 mg/mouse/day) for five consecutive days *via* gavage.

Quantitative reverse transcription PCR (qRT-PCR) analysis. Intracardial perfusion was performed prior to the processing of organs and tissues. RNA was isolated from synovium and other tissues using TRIzol reagent (Invitrogen). The first-strand cDNA was synthesized by using random hexamer primers and RevertAid^{TM}M-MuLV Reverse Transcriptase (Fermentas Life Science). QRT-PCR was performed using an IQ5 multicolor RT-PCR detection system as described previously (20). Primers used are shown in the supplementary table 1.

Flow cytometric analysis. Single-cell suspensions were stained using fluorochrome-conjugated mouse-specific Abs, including APC–anti-CD4 (Biolegend), FITC–anti-CD8 (BD Biosciences), Alexa 700–anti-CD19 (eBioscience), FITC–anti-CD11b (BD Biosciences), FITC–anti-CD11c (BD Biosciences), PE–anti-mouse DR5 (Biolegend), APC–anti-Gr1(Biolegend), PE/Cy7–anti-Ly6C (Biolegend), FITC-anti-IFN-γ (Biolegend), PE-anti-IL-17 (Biolegend), Alexa 647-anti-IL-23p19 (eBioscience), and PE-anti-Foxp3 (eBioscience). Tg chimeric DR5 was stained with biotin–anti human DR5 (Biolegend) followed by Streptavidin eFluor 450 (eBioscience). Prior to staining,

Fc receptors were blocked by anti-mouse CD16/32 (Biolegend). Intracellular and intranuclear staining was performed following manufacturer's instruction (eBioscience). Before intracellular cytokine measurement, cells were stimulated with 25 ng/ml PMA (Sigma) plus 500 ng/ml ionomycin (Sigma) for 2 h with the addition of GolgiStop (BD Biosciences) for an additional 3h. Data were acquired on a BD LSRII flow cytometer and analyzed using FlowJo software (Tree Star, Inc.).

Induction of CIA. CIA was induced and scored in DR5 Tg mice of C57BL/6 background that were 8- to 16-weeks old as described (21). Briefly, mice were immunized by intradermal administration of chicken Type II collagen (Chondrex, Inc.) emulsified in complete Freund's adjuvant (CFA), followed by injection of chicken CII in incomplete Freund's adjuvant (IFA) on day 30 after the primary injection. To ensure a higher incidence of CII arthritis, an adenovirus expressing mouse IL-17 (AdIL-17, $2x10^9$ pfu/mouse, a generous gift from Dr. Jay Kolls) (22) was administered intravenously to all mice 2 days prior to the primary immunization with CII.

TRA-8 treatment of CIA mice. TRA-8 (Daiichi-Sankyo, dissolved in PBS, 0.2 mg per mouse) or IgG1 isotype control was administered *i.v.* or *i.p.* twice/week starting on day 0 (early treatment) or on day 30 (late treatment) until mice were sacrificed.

Histopathologic assessment and immunohistochemical staining. After sacrifice, the knee, ankle, and foot joints were fixed in 4% formaldehyde and then decalcified. Tissue sections (5 μm) were stained with hematoxylin and eosin and examined by light microscopy. Immunohistochemical staining using anti-Mac-3 (clone M3/84, BD Biosciences) was performed as described previously (23). TUNEL assay was performed by using the ApopTag Plus Peroxidase *In Situ* Apoptosis Detection Kit (Millipore), following the manual. Sections were counterstained with hematoxylin or methyl green. Cytospin preparations of LN cells were fixed with 4% formaldehyde. Tyramide signal amplification was carried out according to the manufacturer's instruction (Invitrogen).

***In vivo* imaging of arthritis and apoptosis.** For cathepsin activity determination, mice were injected intravenously with 2 nmol ProSense 750 (ViSen, Bedford, MA) in 150 μl PBS. Twenty-four hours after injection, mice were imaged using the Odyssey Infrared imaging System (LI-COR, Lincoln, Nebraska). For apoptosis detection, a caspase-targeted activity-based probe, AB50–Cy5, was used as described previously (24).

ELISA cytokine measurement. Cytokine levels in sera were measured by ELISA according to the manufacturer's manual (Biolegend).

Statistics. Figures are representative of at least 3 independent experiments. Statistical analyses were performed using two-tailed Student's *t* test, one-way

ANOVA, and bivariate correlation analysis. *P* values <0.05 were considered statistically significant.

RESULTS

Hu/mo-chimeric DR5 proteins and their apoptosis-inducing function upon TRA-8 binding in mouse cells.

Mouse and human DR5 exhibit only ~50% homology at the amino acid level (Figure 1A) and TRA-8, which binds to the extracellular domain of human DR5, however, does not recognize the extracellular domain of mouse DR5. We also observed that the death domain of human DR5 does not initiate the apoptotic cascade in mouse cells. To overcome this obstacle, we generated constructs that express a hu/mo-chimeric DR5 consisting of the extracellular domain of human DR5 with the transmembrane and intracellular domains of mouse DR5 (Figure 1B, Left).

To achieve the desired regulation of hu/mo-chimeric DR5 protein expression, hu/mo DR5 constructs with different regulatory elements were produced that contain the CMV promoter, mouse 1-kb, 3kb DR5 putative promoters, first intron, and 3'-untranslated region (3'-UTR) (Figure 1B, Right). Hu/mo-chimeric DR5 expression was determined by cell-surface flow cytometry using the anti-human DR5 antibody, which recognizes the extracellular domain of human DR5 (Figure 1C). As shown, anti-human DR5 recognized the transfected human (Construct 1) but not mouse DR5 protein (Construct 2). In mouse NIH3T3 cells, the CMV, 1-kb and 3-kb promoter resulted in high expression of the hu/mo-chimeric DR5 (Constructs 3-5) whereas the first intron and 3'UTR of mouse DR5 exhibited negative regulatory effects on hu/mo-chimeric DR5 expression

(Constructs 6, 7). For functional studies, NIH 3T3 mouse cells were transfected with these constructs (Figure 1D). TRA-8 (1 μg/ml) was added 24 h after transfection, followed by overnight incubation. The ATPLite assay was used to measure the cell viability. TRA-8 did not decrease viability in cells transfected with the full-length human or mouse DR5 driven by the CMV promoter, which lack either the mouse death domain that initiates apoptotic signaling or the human extracellular domain that binds TRA-8 (Constructs 1 and 2, Figure 1D). However, in cells transfected with the chimeric DR5, significant reduced cell viability by TRA-8 was detected, with the 3-kb chimeric DR5 construct resulted in the highest apoptosis inducing effect by TRA-8 (Constructs 3-5, Figure 1D). Addition of the first intron and the 3'-UTR reduced the TRA-8 killing effect (Figure 1D). Thus, the chimeric DR5 regulated by the 3-kb promoter (Construct 5, Figure 1B, C, and D) is the optimal construct for DR5 expression and TRA-8-mediated apoptosis and was selected for generation of Tg mice.

Expression of hu/mo-chimeric DR5 and its apoptosis-inducing function in hu/mo DR5 Tg^{+} Ubc.Cre mice.

In order to enable temporal and spatial expression of the chimeric DR5, a *Floxed*-STOP was inserted between the 3-kb promoter and the chimeric DR5. Founder DR5 Tg mice were crossed with Ubc.Cre mice, which exhibit strong tamoxifen-inducible Cre expression ubiquitously. To determine if the tissue distribution of the chimeric *Dr5* correlates with that of endogenous mouse *Dr5*, the expression of chimeric *Dr5* and mouse endogenous *Dr5* in tissues harvested

from tamoxifen treated DR5 Ubc.Cre mice was determined (Figure 2A). Tamoxifen treatment induced the expression of the hu/mo-chimeric DR5 Tg in various tissues, including the lymph nodes (LN), brain, lung, spleen, and kidney and the expression pattern exhibited a significant correlation with that of the endogenous mouse DR5 (Figure 2A). Western blot analysis indicated that the hu/mo DR5 Tg protein expression correlated with the mRNA expression with high level of protein detected in the LN, spleen and lung (Data not shown).

To examine the chimeric DR5 expression in different immune cells and TRA-8 induced apoptosis, CIA was induced in these mice. Chicken type II collagen (cCII) induces arthritis in approximately 60–70% of mice with the H-2^b background (25). Prior to injection of cCII, we administered mice with an adenovirus that expresses IL-17 (AdIL-17) to increase the incidence of arthritis and thus facilitate the evaluation of the therapeutic effects of TRA-8 (22). In the draining LN of the mice with CIA (two months after primary CII injection), the expression of the hu/mo-chimeric DR5 was highest in the $CD11b^+Gr\text{-}1^+$ granulocytes and $CD11b^+Ly6C^+$ inflammatory macrophages, with lower expression on $CD4^+$ and $CD8^+$ T cells, and minimal expression on $CD19^+$ B cells (Figure 2B). Importantly, both early and late TRA-8 treatment (0.2 mg twice/week) reduced the percentage of $CD11b^{high}$ -activated macrophages in the LN by ~50–60% (Figure 2C), suggesting that TRA-8 can potentially suppress the frequency of macrophages during an active inflammatory stage in CIA.

To further assess the effects of TRA-8 on the macrophages, a single-cell suspension prepared from the draining inguinal lymph nodes of the cCII-induced hu/mo-chimeric DR5 Tg^+ Ubc.Cre mice without *in vivo* TRA-8 treatment was stimulated with LPS (5 μg/ml) for 2 days and then treated with or without TRA-8 for an additional 2 days. As shown in Figure 2D, for LPS-stimulated macrophages obtained from hu/mo-chimeric DR5 Tg^+ Ubc.Cre mice, thymidine incorporation was significantly lower in TRA-8-treated than untreated mice.

TRA-8 treatment prevents the development of, and ameliorates established arthritis in hu/mo DR5 Tg^+ Ubc.Cre mice.

After CIA induction (Figure 3A and B, arrows), both the isotype-treated hu/mo DR5 Tg^+ Ubc.Cre (DR5 Tg^+) mice and the control DR5 Tg^- Ubc.Cre (DR5 Tg^-) mice developed joint swelling and erythema indicated by the arthritis score (Figure 3A and B, gray squares). Early TRA-8 treatment (0.2 mg twice/week) of the hu/mo-chimeric DR5 Tg^+ Ubc.Cre mice resulted in a significant reduction in the early-stage arthritis, as well as the late-stage arthritis that was associated with the CII boost (Figure 3A, filled circles). Moreover, initiation of the TRA-8 treatment (0.2 mg twice/week) 2 days before the CII boost significantly inhibited the late phase of CIA (Figure 3A, open circles). In contrast, TRA-8 treatment of the control DR5 Tg^- Ubc.Cre mice did not affect the development of arthritis in response to either the primary or secondary CII injection (Figure 3B). Histopathologic analysis of the joints from cCII-injected hu/mo-chimeric DR5 Tg^+ Ubc.Cre mice 2 months after TRA-8 treatment revealed a dramatic reduction in

the severity of synovial hyperplasia (H), and bone erosion (E), as well as significant attenuation of inflammatory cell infiltration in the joints (Figure 3C, left panels) compared to DR5 Tg^- control (Figure D, left panels). Immunohistochemical analysis of the synovium revealed that the numbers of Mac-3^+ macrophages (M) were much lower in the TRA-8-treated, CII-injected hu/mo-chimeric DR5 Tg^+ Ubc.Cre mice than their untreated counterparts (Figure 3C and D, right panel).

TRA-8 treatment specifically eliminates inflammatory macrophages and ameliorates established arthritis in hu/mo DR5 Tg^+ LysM.Cre mice.

To test whether targeted depletion of macrophages with TRA-8 is feasible *in vivo*, we restricted expression of the chimeric DR5 to myeloid lineage cells by crossing the *Floxed*-STOP chimeric DR5 Tg mice with mice in which Cre is driven by the lysozyme M (Lys.M) promoter (26). CIA was induced as described above. At day 60, FACS analysis showed that $CD11b^+$ macrophages from the draining LN of hu/mo-chimeric DR5 in DR5 Tg^+ LysM.Cre (DR5 Tg^+) mice exhibited increased cell surface binding to anti-human DR5 compared with that of the control mice (Figure 4A, upper panel). A similar result was also confirmed by cytospin (Figure 4A, lower panel). There was a very low frequency of $CD4^+$, $CD8^+$ T cells and $CD19^+$ B cells that expressed hu/mo-chimeric DR5 (<1%) in these mice (Figure 4B). TRA-8 treatment of these mice reduced the percentage of $CD11b^+$ macrophages from 4.3% to 1.5% (Figure 4C), whereas the TRA-8 depletion effect was not significant in DR5 Tg^- mice (Figure 4C). Within the

$CD11b^+$ cells, the percentage of the $Ly6C^+$ inflammatory macrophage subpopulation was reduced from 3.1% to 0.75% (Figure 4D) and this effect was not significant in DR5 Tg^- mice. TRA-8 treatment did not change in the percentage of total $CD4^+$ and $CD8^+$ T cells, $CD19^+$ B cells, or $CD11c^+$ dendritic cells in all these four groups of mice (data not shown).

TRA-8-induced apoptosis was assessed by a non-invasive *in vivo* imaging method and a TUNEL staining. LysM.Cre hu/mo-chimeric DR5 Tg^+ and control LysM.Cre mice were induced to develop CIA. At 8 weeks after induction, baseline-levels of caspase activity were measured *in vivo* using the caspase imaging probe AB50–Cy5 (24). Mice were then treated with TRA-8 (0.2 mg on day 0 and day 3) and apoptosis imaging was repeated on the same mice. Apoptosis reached the peak 6 days after the first dose of TRA-8 administration (Figure 5A, right panel and B). There was a significant increase in the caspase probe signal in mice with arthritis post- compared with pre-TRA-8 treatment (Figure 5A, right panel and 5B). Our result demonstrated that TRA-8 can induce apoptosis *in vivo* in the joints of arthritic mice.

Apoptosis analysis by TUNEL assay was carried out on joint sections of the same mice after acute TRA-8 treatment, as described above. At this early time point after short term TRA-8 treatment, there was no significantly difference in synovial hyperplasia (H), bone erosion (E), and macrophage infiltration (M) between LysM.Cre hu/mo-chimeric DR5 Tg^+ (Tg $DR5^+$) and control LysM.Cre

DR5$^-$ Tg (Tg DR5$^-$) mice (Figure 5C, left and middle panels). There was a significantly increased TUNEL staining (TU) after short term TRA-8 treatment in the hu/mo-chimeric DR5 Tg$^+$ mice but not in control DR5 Tg$^-$ mice (Figure 5C, right panels). Serial section staining indicated that the TUNEL staining was most prominent in macrophages (M) within the intima and sublining of the synovium (Figure 5C, right panels). Apoptosis of macrophages and fibroblasts was also quantified by calculating the percentage of apoptotic cells in the Mac-3$^+$ and Mac-3$^-$ regions (Figure 5D).

Following establishment of CIA, TRA-8 treatment (0.2mg twice/week) significantly attenuated the severity of the arthritis in the hu/mo-chimeric DR5 Tg$^+$ LysM.Cre (Tg DR5$^+$) mice (Figure 6A, upper panel), but not in control DR5 Tg$^-$ LysM.Cre (Tg DR5$^-$) mice (Figure 6A, lower panel), suggesting that targeted depletion of macrophages can ameliorate CIA. Production of high levels of cysteine cathepsins is clinically associated with arthritis severity (27). Assessment of cathepsin activity using the ProSense 750^{TM} protease probe confirmed high levels of activity in the ankles, tarsal joints, and digits of control DR5 Tg$^-$ LysM.Cre mice with and without TRA-8 treatment, and in hu/mo-chimeric DR5 Tg$^+$ LysM.Cre mice that were not treated with TRA-8. In marked contrast, only minimal protease activity was found in the TRA-8-treated hu/mo-chimeric DR5 Tg$^+$ LysM.Cre mice (Figure 6B, C). Histopathologic analysis of the joints from cCII-injected chimeric DR5 Tg mice (Figure 6D, left panels) treated with TRA-8 for one month revealed a dramatic reduction in the severity of

synovial hyperplasia (H), inflammatory cell infiltration, bone erosion (E) in the joints, and a significant decrease in $Mac3^+$ macrophages (M) in synovium compared to DR5 Tg^- control mice (Figure 6D, right panels). TRAP staining (TR) further indicated that TRA-8 treatment also lead to the reduced activity of osteoclasts in the joints (Figure 6D).

TRA-8 treatment decreases the expression of pro-inflammatory cytokines and exhibits immunomodulatory effects in hu/mo DR5 Tg^+ LysM.Cre mice.

To further investigate the immune response regulated by the depletion of inflammatory macrophages, sera and synovial cytokines were assessed on day 60. TRA-8 treatment significantly reduced the protein levels of IL-6 and IL-17A in the sera (Figure 7A) as well as *Tnfa, Il6, Il23a(p19)* and *Il17a* transcripts in the joints of DR5Tg^+ LysM.Cre mice treated with TRA-8 (Figure 7B) compared to control DR5Tg^- mice with CIA. In the $CD11b^+$ cell population from the draining LN, the percentage of IL-23^+ inflammatory macrophages was reduced from 5.8% to 0.2% (Figure 7C), which is consistent with the observation that the expression of *Irf5*, a signature transcription factor of inflammatory macrophages (28), is also reduced in the synovium of the TRA-8 treated mice (Figure 7B). IL-23 is a pro-inflammatory cytokine that has been proposed to play a central role in the development of arthritis (29-31), which is related to the dysregulated balance between IL-23/Th17 axis and regulatory T cells (Tregs) (32). We further identified that TRA-8 treatment can restrain Th17 while promoting Tregs cell development. Th17 cells were reduced from 2.9% to 1.4% whereas Tregs were increased from

3.9% to 6.3% (Figure 7D) in the DR5Tg^{+} LysM.Cre mice treated with TRA-8 compared with the control DR5Tg^{-} mice with CIA. Consistent with this, there were decreased expression of the *Il-17a* and increased expression of *Foxp3* in the synovium (Figure 7B). IFNγ-producing Th1 cells were also reduced by TRA-8 treatment in these mice (Figure 7D).

DISCUSSION

The present results are the first to show that *in vivo* administration of TRA-8 can directly induce apoptosis of a subpopulation of macrophages and attenuate CIA. The predominant cell types targeted by TRA-8 therapy are a subpopulation of inflammatory macrophages which produce high levels of cytokines, including TNF-α and IL-6 (33). TRA-8 therapy has a novel cell depletion mechanism of directly triggering apoptosis of the targeted cells. TRA-8 and its humanized version, tigatuzumab (CS1008), have been shown to be effective in elimination of tumor cells in xenograft cancer models and well-tolerated in a phase I clinical trail (34, 35).

TRA-8 exhibits higher selectivity than TRAIL and it does not recognize mouse MK (14). The existing anti-mouse MK monoclonal antibody (MD5-1) is not efficacious in inducing apoptosis without cross-linkers (19). Furthermore, we have found that the neither human DR5 nor mouse MK initiated TRA-8-mediated apoptotic cascades in mouse cells (Figure 1D). To investigate the efficacy and the mechanism of TRA-8 therapy in mouse models, we generated a chimeric hu/mo-chimeric DR5 Tg comprised of the extracellular domain of human DR5 and the transmembrane and intracellular domains of mouse MK with regulatory elements. The expression of the chimeric DR5 was comparable to endogenous mouse MK. We observed that the chimeric DR5 is predominantly expressed in $CD11b^+$ macrophages of DR5 Tg mice crossed with both Ubc.Cre and LysM.Cre

mice after induction of CIA. This suggested that the mouse MK 3-kb promoter is active in macrophage during arthritis pathogenesis.

DR5 is broadly expressed in most human tissues (36, 37). In tumors, its expression is highest in melanoma and lung cancers (36). Although human DR5 is widely expressed, anti-DR5 treatment induced apoptosis only occurs in selected cells (38). The present study indicated the high selectivity of TRA-8-mediated killing in $CD11b^{hi}$ $Ly6C^{+}$ macrophages. Ly6C is a monocyte/macrophage differentiation antigen regulated by interferon-γ (39), which has been shown to facilitate apoptosis signaling in macrophages and cancer cells (40, 41). Inflammatory macrophages express much higher levels of Ly6C distinguished from those residing normally in the tissues (42). In CIA and K/BxN serum transfer-induced arthritis, reduction of $Ly6C^{+}$ synovial macrophages has been associated with GM-CSF blockade and reduction in disease severity (43), suggesting that $Ly6C^{hi}$ macrophages are associated with GM-CSF-mediated arthritis response. Our results suggest that TRA-8 treatment can shape the heterogeneity of macrophages, leading to the homeostasis of the myelomonocytic cells in the inflammatory conditions.

One of the major advantages of DR5 is the inflammation-dependent selectivity which is reflected by the fact that while the chimeric DR5 was found to be mainly expressed by macrophages, inflammatory $Ly6C^{+}$ $CD11b^{+}$ macrophages are more susceptible to DR5 mediated apoptosis. This suggested

that our approach of using TRA-8 can selectively deplete inflammatory macrophages while sparing the anti-inflammatory macrophages. It has been reported that one single dosage of intraarticular administration of clodronate liposomes leads to macrophage depletion in the synovium of RA patients (44), however, such therapy may not be safe for systemic administration and depletion of macrophages based on their phagocytotic capacity will be difficult in terms of specificity of killing and regulation of activity (45).

Dysregulated IL-23/Th17 axis and Tregs have been implicated in the pathogenesis of RA. Interactions between CD4 T cells and macrophages have been shown to be important for polarization of both lineages of cells (30, 46, 47). Recently, it has been reported that human Tregs can be converted to Th17 cells in the context of inflammatory signals and this differentiation process can be enhanced by IL-1β, IL-23, and IL-21 (48). We have determined the polarization condition of CD4 T cells in these mice after macrophage depletion by TRA-8. Interestingly, we found that there was a significant decrease in the frequency of Th17 and Th1 CD4 T cells in the LN isolated from the TRA-8 treated DR5 Tg^+ LysM.Cre mice compared to control TRA-8 treated DR5 Tg^- LysM.Cre mice with CIA. In contrast, the frequency of Tregs in the LN of DR5 Tg^+ LysM.Cre mice was nearly 2 fold higher than that in the DR5 Tg^- LysM.Cre mice. Our results suggest that TRA-8, *via* diminishing the frequency of IL-23^+ M1 macrophages, can indirectly regulate the balance of pro-inflammatory versus anti-inflammatory effector CD4 T cells.

In conclusion, the results of the present study indicate that the anti-human DR5 antibody TRA-8 can specifically eliminate inflammatory macrophages leading to the rebalance of the IL-23/Th17 axis and Tregs and resolution of arthritis in a mouse arthritis model, which suggests that anti-human DR5 can be developed into a novel biologic agent for the therapy of RA and other macrophage-mediated inflammatory diseases or autoimmune diseases.

REFERENCES

1. Kinne RW, Brauer R, Stuhlmuller B, Palombo-Kinne E, Burmester GR. Macrophages in rheumatoid arthritis. Arthritis Res 2000;2(3):189-202.

2. Pap T, Muller-Ladner U, Gay RE, Gay S. Fibroblast biology. Role of synovial fibroblasts in the pathogenesis of rheumatoid arthritis. Arthritis Res 2000;2(5):361-7.

3. Lundy SK, Sarkar S, Tesmer LA, Fox DA. Cells of the synovium in rheumatoid arthritis. T lymphocytes. Arthritis Res Ther 2007;9(1):202.

4. Moreland LW, Pratt PW, Mayes MD, Postlethwaite A, Weisman MH, Schnitzer T, et al. Double-blind, placebo-controlled multicenter trial using chimeric monoclonal anti-CD4 antibody, cM-T412, in rheumatoid arthritis patients receiving concomitant methotrexate. Arthritis Rheum 1995;38(11):1581-8.

5. Edwards JC, Cambridge G. Sustained improvement in rheumatoid arthritis following a protocol designed to deplete B lymphocytes. Rheumatology (Oxford) 2001;40(2):205-11.

6. Cohen SB, Emery P, Greenwald MW, Dougados M, Furie RA, Genovese MC, et al. Rituximab for rheumatoid arthritis refractory to anti-tumor necrosis factor therapy: Results of a multicenter, randomized, double-blind, placebo-controlled, phase III trial evaluating primary efficacy and safety at twenty-four weeks. Arthritis Rheum 2006;54(9):2793-806.

7. Calero I, Nieto JA, Sanz I. B cell therapies for rheumatoid arthritis: beyond B cell depletion. Rheum Dis Clin North Am 2010;36(2):325-43.

8. Maruotti N, Cantatore FP, Crivellato E, Vacca A, Ribatti D. Macrophages in rheumatoid arthritis. Histol Histopathol 2007;22(5):581-6.

9. Kinne RW, Stuhlmuller B, Burmester GR. Cells of the synovium in rheumatoid arthritis. Macrophages. Arthritis Res Ther 2007;9(6):224.

10. Szekanecz Z, Koch AE. Macrophages and their products in rheumatoid arthritis. Curr Opin Rheumatol 2007;19(3):289-95.

11. McInnes IB, Leung BP, Liew FY. Cell-cell interactions in synovitis. Interactions between T lymphocytes and synovial cells. Arthritis Res 2000;2(5):374-8.

12. Kiener HP, Watts GF, Cui Y, Wright J, Thornhill TS, Skold M, et al. Synovial fibroblasts self-direct multicellular lining architecture and synthetic function in three-dimensional organ culture. Arthritis Rheum 2010;62(3):742-52.

13. Egan PJ, van Nieuwenhuijze A, Campbell IK, Wicks IP. Promotion of the local differentiation of murine Th17 cells by synovial macrophages during acute inflammatory arthritis. Arthritis Rheum 2008;58(12):3720-9.

14. Ichikawa K, Liu W, Zhao L, Wang Z, Liu D, Ohtsuka T, et al. Tumoricidal activity of a novel anti-human DR5 monoclonal antibody without hepatocyte cytotoxicity. Nat Med 2001;7(8):954-60.

15. MacFarlane M, Ahmad M, Srinivasula SM, Fernandes-Alnemri T, Cohen GM, Alnemri ES. Identification and molecular cloning of two novel receptors for the cytotoxic ligand TRAIL. J Biol Chem 1997;272(41):25417-20.

16. Bellail AC, Qi L, Mulligan P, Chhabra V, Hao C. TRAIL agonists on clinical trials for cancer therapy: the promises and the challenges. Rev Recent Clin Trials 2009;4(1):34-41.

17. Yagita H, Takeda K, Hayakawa Y, Smyth MJ, Okumura K. TRAIL and its receptors as targets for cancer therapy. Cancer Sci 2004;95(10):777-83.

18. Ichikawa K, Liu W, Fleck M, Zhang H, Zhao L, Ohtsuka T, et al. TRAIL-R2 (DR5) mediates apoptosis of synovial fibroblasts in rheumatoid arthritis. J Immunol 2003;171(2):1061-9.

19. Takeda K, Yamaguchi N, Akiba H, Kojima Y, Hayakawa Y, Tanner JE, et al. Induction of tumor-specific T cell immunity by anti-DR5 antibody therapy. J Exp Med 2004;199(4):437-48.

20. Hsu HC, Yang P, Wu Q, Wang JH, Job G, Guentert T, et al. Inhibition of the catalytic function of activation-induced cytidine deaminase promotes apoptosis of germinal center B cells in BXD2 mice. Arthritis Rheum 2011;63(7):2038-48.

21. Inglis JJ, Simelyte E, McCann FE, Criado G, Williams RO. Protocol for the induction of arthritis in C57BL/6 mice. Nat Protoc 2008;3(4):612-8.

22. Lubberts E, van den Bersselaar L, Oppers-Walgreen B, Schwarzenberger P, Coenen-de Roo CJ, Kolls JK, et al. IL-17 promotes bone erosion in murine collagen-induced arthritis through loss of the receptor activator of NF-kappa B ligand/osteoprotegerin balance. J Immunol 2003;170(5):2655-62.

23. Wu Y, Liu J, Feng X, Yang P, Xu X, Hsu HC, et al. Synovial fibroblasts promote osteoclast formation by RANKL in a novel model of spontaneous erosive arthritis. Arthritis Rheum 2005;52(10):3257-68.

24. Edgington LE, Berger AB, Blum G, Albrow VE, Paulick MG, Lineberry N, et al. Noninvasive optical imaging of apoptosis by caspase-targeted activity-based probes. Nat Med 2009;15(8):967-73.

25. Inglis JJ, Criado G, Medghalchi M, Andrews M, Sandison A, Feldmann M, et al. Collagen-induced arthritis in C57BL/6 mice is associated with a robust and sustained T-cell response to type II collagen. Arthritis Res Ther 2007;9(5):R113.

26. Clausen BE, Burkhardt C, Reith W, Renkawitz R, Forster I. Conditional gene targeting in macrophages and granulocytes using LysMcre mice. Transgenic Res 1999;8(4):265-77.

27. Hansen T, Petrow PK, Gaumann A, Keyszer GM, Eysel P, Eckardt A, et al. Cathepsin B and its endogenous inhibitor cystatin C in rheumatoid arthritis synovium. J Rheumatol 2000;27(4):859-65.

28. Krausgruber T, Blazek K, Smallie T, Alzabin S, Lockstone H, Sahgal N, et al. IRF5 promotes inflammatory macrophage polarization and TH1-TH17 responses. Nat Immunol 2011;12(3):231-8.

29. Cornelissen F, van Hamburg JP, Lubberts E. The IL-12/IL-23 axis and its role in Th17 cell development, pathology and plasticity in arthritis. Curr Opin Investig Drugs 2009;10(5):452-62.

30. Paradowska-Gorycka A, Grzybowska-Kowalczyk A, Wojtecka-Lukasik E, Maslinski S. IL-23 in the pathogenesis of rheumatoid arthritis. Scand J Immunol 2010;71(3):134-45.

31. Hillyer P, Larche MJ, Bowman EP, McClanahan TK, de Waal Malefyt R, Schewitz LP, et al. Investigating the role of the interleukin-23/-17A axis in rheumatoid arthritis. Rheumatology (Oxford) 2009;48(12):1581-9.

32. Nistala K, Wedderburn LR. Th17 and regulatory T cells: rebalancing pro- and anti-inflammatory forces in autoimmune arthritis. Rheumatology (Oxford) 2009;48(6):602-6.

33. Dunay IR, Damatta RA, Fux B, Presti R, Greco S, Colonna M, et al. Gr1(+) inflammatory monocytes are required for mucosal resistance to the pathogen Toxoplasma gondii. Immunity 2008;29(2):306-17.

34. Kim H, Morgan DE, Zeng H, Grizzle WE, Warram JM, Stockard CR, et al. Breast tumor xenografts: diffusion-weighted MR imaging to assess early therapy with novel apoptosis-inducing anti-DR5 antibody. Radiology 2008;248(3):844-51.

35. Forero-Torres A, Shah J, Wood T, Posey J, Carlisle R, Copigneaux C, et al. Phase I trial of weekly tigatuzumab, an agonistic humanized monoclonal antibody targeting death receptor 5 (DR5). Cancer Biother Radiopharm 2010;25(1):13-9.

36. Daniels RA, Turley H, Kimberley FC, Liu XS, Mongkolsapaya J, Ch'En P, et al. Expression of TRAIL and TRAIL receptors in normal and malignant tissues. Cell Res 2005;15(6):430-8.

37. Spierings DC, de Vries EG, Vellenga E, van den Heuvel FA, Koornstra JJ, Wesseling J, et al. Tissue distribution of the death ligand TRAIL and its receptors. J Histochem Cytochem 2004;52(6):821-31.

38. Amm HM, Zhou T, Steg AD, Kuo H, Li Y, Buchsbaum DJ. Mechanisms of Drug Sensitization to TRA-8, an Agonistic Death Receptor 5 Antibody, Involve Modulation of the Intrinsic Apoptotic Pathway in Human Breast Cancer Cells. Mol Cancer Res 2011;9(4):403-417.

39. Jutila MA, Kroese FG, Jutila KL, Stall AM, Fiering S, Herzenberg LA, et al. Ly-6C is a monocyte/macrophage and endothelial cell differentiation antigen regulated by interferon-gamma. Eur J Immunol 1988;18(11):1819-26.

40. Kohara H, Kitaura H, Fujimura Y, Yoshimatsu M, Morita Y, Eguchi T, et al. IFN-gamma directly inhibits TNF-alpha-induced osteoclastogenesis in vitro and in vivo and induces apoptosis mediated by Fas/Fas ligand interactions. Immunol Lett 2011;137(1-2):53-61.

41. Shin EC, Ahn JM, Kim CH, Choi Y, Ahn YS, Kim H, et al. IFN-gamma induces cell death in human hepatoma cells through a TRAIL/death receptor-mediated apoptotic pathway. Int J Cancer 2001;93(2):262-8.

42. Chan J, Leenen PJ, Bertoncello I, Nishikawa SI, Hamilton JA. Macrophage lineage cells in inflammation: characterization by colony-stimulating factor-1 (CSF-1) receptor (c-Fms), ER-MP58, and ER-MP20 (Ly-6C) expression. Blood 1998;92(4):1423-31.

43. Cook AD, Turner AL, Braine EL, Pobjoy J, Lenzo JC, Hamilton JA. Regulation of systemic and local myeloid cell subpopulations by bone marrow

cell-derived granulocyte-macrophage colony-stimulating factor in experimental inflammatory arthritis. Arthritis Rheum 2011;63(8):2340-51.

44. Barrera P, Blom A, van Lent PL, van Bloois L, Beijnen JH, van Rooijen N, et al. Synovial macrophage depletion with clodronate-containing liposomes in rheumatoid arthritis. Arthritis Rheum 2000;43(9):1951-9.

45. Van Rooijen N. The liposome-mediated macrophage 'suicide' technique. J Immunol Methods 1989;124(1):1-6.

46. Sato K, Suematsu A, Okamoto K, Yamaguchi A, Morishita Y, Kadono Y, et al. Th17 functions as an osteoclastogenic helper T cell subset that links T cell activation and bone destruction. J Exp Med 2006;203(12):2673-82.

47. Notley CA, Inglis JJ, Alzabin S, McCann FE, McNamee KE, Williams RO. Blockade of tumor necrosis factor in collagen-induced arthritis reveals a novel immunoregulatory pathway for Th1 and Th17 cells. J Exp Med 2008;205(11):2491-7.

48. Koenen HJ, Smeets RL, Vink PM, van Rijssen E, Boots AM, Joosten I. Human CD25highFoxp3pos regulatory T cells differentiate into IL-17-producing cells. Blood 2008;112(6):2340-52.

AUTHOR CONTRIBUTIONS

J.L., H-C. H., H. L. and J.D.M. designed experiments, analyzed data, and wrote the manuscript. J.L. designed, generated, and tested all constructs used for this work. J.L. and PA. Y. paired, bred, and genotyped all mice used for this study. J.L., PA. Y., and Q.W. carried out all *in vivo* and *in vitro* experiments. R.P.K designed experiments and was involved in interpretation of data. L.E. and M.B. provided the AB50–Cy5 apoptosis imaging probes, assisted the in vivo apoptosis imaging analysis, and were involved in writing the manuscript. J.D.M. directed all of the experiments.

ACKNOWLEDGEMENTS

We thank Mr. Larry Johnson and Mr. Jingju Zhang at the UAB Arthritis and Musculoskeletal Disease Center – Gene Targeting Core Facility for generation of the human/mouse DR5 transgenic mice (P30 AR48311). We thank Ms. Enid Keyser of the UAB Arthritis and Musculoskeletal Disease Center Analytic and Preparative Cytometry Facility for operating the FACS instrument (P30 AR48311). Confocal imaging was carried out at the UAB Arthritis and Musculoskeletal Disease Center High Resolution Imaging Facility (P30 AR48311). Joint processing and sections were carried out at the UAB Center for Metabolic Bone Disease Core Laboratory. AdIL-17 is a generous gift from Dr. Jay Kolls at the Louisiana State University – Health Sciences Center. Dr. Fiona Hunter provided editorial assistance in the preparation of the manuscript.

FIGURE LEGENDS

Figure 1. Human, mouse and chimeric DR5 and their expression and function in inducing apoptosis by TRA-8. **A,** Amino acid alignment of human and mouse DR5. Junction between human and mouse DR5 in the chimeric molecule, transmembrane, and death domain are as indicated. **B,** Schematic diagram representing the human, mouse and chimeric DR5 (left), and human, mouse and chimeric DR5 constructs generated with different promoters and regulatory elements (right). **C,** FACS analysis of cell surface expression of DR5 recognized by an anti-human DR5 antibody in NIH3T3 cells transiently transfected with the indicated constructs. Percentage of the hu/mo $DR5^+$ cells was shown. $N \geq 3$. * $P < 0.05$ versus result from construct 1. **D,** TRA-8 mediated killing in NIH3T3 transiently transfected with the indicated constructs. Cell viability was determined using the ATPLite assay. For panels C and D**,** the data represent the mean ± s.e.m. (n ≥ 3). Hu, human; mo, mouse; chim, chimeric. * $P < 0.05$ and ** $P < 0.01$ versus isotype control.

Figure 2. Hu/mo-chimeric Tg DR5 expression and function in Ubc.Cre DR5 Tg mice. **A,** Real-time PCR analysis of the chimeric *DR5* expression in the indicated tissues obtained from the Ubc.Cre DR5 double-positive transgenic mice after induction of Cre expression by tamoxifen. Expression is represented as the ratio of copy numbers of chimeric *Dr5* or endogenous mouse *Dr5* to those of *Gapdh*. The correlation R^2 and correlation *P* value are shown in the upper-right of the panel. **B,** Transgenic chimeric DR5 cell surface expression on different immune

cells was analyzed by FACS (left panels). The chimeric DR5 expression is representative of three experiments (right panels). **C,** The percentage of $CD11b^{high}$ spleen macrophages from mice with and without TRA-8 treatment (0.2 mg, *i.v.*, twice/week for 2 months) was determined by FACS. Data represent the mean ± s.e.m. (n ≥ 3). **D,** Proliferation of LPS-stimulated spleen cells from DR5 Tg^- Ubc.Cre and hu/mo DR5 Tg^+ Ubc.Cre mice treated with TRA-8 or isotype control antibody was determined using the [^{3}H]-thymidine incorporation assay (n ≥ 3). * $P < 0.05$ versus isotype control.

Figure 3. TRA-8 treatment prevents the development and attenuates the severity of CIA in hu/mo-chimeric DR5 Tg^+ Ubc.Cre mice. CIA was induced in the indicated DR5 Tg^+ (**A**) and DR5 Tg^- mice (**B**) as described in detail in the methods section. Chicken type II collagen emulsified in CFA and IFA was administered intradermally on day 0 and day 32 respectively (arrows). Early and late TRA-8 treatment (0.2 mg/mouse, once per week) was initiated on day 0 and day 30 respectively (arrow heads) and continued until sacrifice. Clinical scores (0-3 per paw; n=6 per group) were assessed daily until the mice were sacrificed. Data are presented as mean arthritis score ± s.e.m.. ** $P < 0.01$ versus TRA-8-treated groups at the same time point. **C** and **D,** Representative H&E and Mac-3 immunohistochemical staining of the knee joint sections from a TRA-8 treated hu/mo DR5 Tg^+ Ubc.Cre (**C**) or a TRA-8 treated DR5 Tg^- Ubc.Cre (**D**) mouse. The magnification of the objective lens used to acquire the indicated images is

shown in the left. E, erosion; H, hyperplasia; M, macrophages, (Scale bar, 100 μm).

Figure 4. Expression of hu/mo-chimeric DR5 in macrophages and selective depletion by TRA-8 in hu/mo DR5 Tg^+ LysM.Cre mice with CIA. CIA was induced as described in the methods section. A group of mice were treated with TRA-8 (0.2 mg/mouse, *i.v.*, twice/week) until analysis at day 60 post primary cCII injection. **A,** Flow cytometry analysis of the expression of Tg DR5 as indicated by cell surface binding to an anti-human DR5 antibody on $CD11b^+$ cells from the draining LN (upper panels). Chimeric Tg DR5 expression on $CD11b^+$ cells by immunofluoresence staining of CD11b and hu/mo-chimeric DR5 on cells prepared by cytospin without cell permeabilization (lower panels). Chimeric Tg DR5 was detected using the Tyramide Signal Amplification (TSA) technique. **B,** Flow cytometry analysis of the expression of Tg DR5 by cell surface binding to an anti-human DR5 antibody on the indicated cell types from the draining LN. **C** and **D,** TRA-8 treatment depleted $CD11b^+$ macrophages and $CD11b^+Ly6C^+$ inflammatory macrophages from draining LN from the indicated groups of mice by dot plot (left) and bar graph (right) analysis. Data represent the mean ± s.e.m. ($n \geq 3$). * $P < 0.05$ and ** $P < 0.01$ between the indicated comparisons.

Figure 5. Apoptosis induced by TRA-8 in the joints of hu/mo-chimeric DR5 Tg^+ LysM. Cre mice with CIA. **A,** *In vivo* imaging of TRA-8 induced apoptosis in joints. **B,** Quantitation of the imagines. DR5 Tg^+ LysM.Cre and control LysM.Cre

mice were induced to develop CIA. At 8 week after induction, baseline levels of the caspase activity were measured using the caspase-targeted activity based probe AB50-Cy5 (left panel). Mice were then treated with TRA-8 (0.2 mg, day 0 and 3) and apoptosis imaging using AB50-Cy5 was performed on the same mice on day 6 after initiating TRA-8 treatment (right panel). **C,** Immediately after the second AB50-Cy5 imaging, the joints were removed, fixed and processed for H.&E. (left), Mac-3 staining (middle, counterstained with methyl green), and TUNEL (right, counterstained with hematoxyline). **D,** Quantitative analysis of the $TUNEL^+$ cells of the indicated cell types in synovium. The values on the Y-axis represent the percentages of TUNEL-positive cells of the indicated cell types. Five randomly chosen fields of synovium were evaluated for each section. E, erosion; H, hyperplasia; M, macrophages, and TU, TUNEL. Scale bar, 100 μm. Data represent mean ± s.e.m. (n ≥ 3). ** $P < 0.01$ between the indicated comparisons.

Figure 6. TRA-8 treatment ameliorates the severity of CIA in hu/mo-chimeric DR5 Tg^+ LysM.Cre mice. **A,** CIA was induced in hu/mo DR5 Tg^+ LysM.Cre (upper panel) and control DR5 Tg^- LysM.Cre mice (lower panel). Arrows indicate the intradermal injection of chicken type II collagen on day 0 and 30. TRA-8 treatment was initiated on day 28 (arrow heads). Clinical scores (n = 6 per group) were assessed until the mice were sacrificed on day 60. Data are presented as the mean clinical score ± s.e.m. * $P < 0.05$ and ** $P < 0.01$ versus TRA-8 treated group at the indicated time point. **B,** Cathepsin activity in joints was measured by

in vivo imaging using the NIRF-probe ProSense 750. **C,** Quantitative analysis of ProSense 750 intensity. Data are presented as the mean ± s.e.m. * $P < 0.05$ between the indicated comparisons. **D,** Histological assessment of representative knee joints from TRA-8-treated DR5 Tg^+ LysM.Cre DR5 (left panels) and DR5 Tg^- LysM.Cre mice (right panels), which included H&E , Mac-3, and TRAP staining as indicated (scale bar: 100 μm). Both groups were treated with TRA-8 weekly for one month. E, erosion; H, hyperplasia; M, macrophages, and TR, TRAP.

Figure 7. TRA-8 treatment decreases the expression of pro-inflammatory cytokines and exhibits immunomodulatory effects in hu/mo DR5 Tg^+ LysM.Cre mice. CIA was induced in hu/mo DR5 Tg^+ LysM.Cre and control DR5 Tg^- LysM.Cre mice as described in the methods section. TRA-8 treatment was initiated on day 28 until analysis at day 60 post primary cCII injection. **A,** Sera levels of IL-6 and IL-17A of indicated mice with TRA-8 treatment were analyzed by ELISA. **B,** Absolute copy numbers of *Tnfa, Il6, Il17, Il23(p19), Irf5* and *Foxp3* of synovium of the indicated mice were determined by qRT-PCR and represented as copy number $x10^5$/*Gapdh*. **C**, Percentage of IL-23^+ $CD11b^+$ macrophages from the draining LN of the indicated mice treated with TRA-8 on day 60 ($CD11b^+$ gated) was determined by flow cytometry. **D**, Percentage of Th17 (IL-17^+) and Th1 (IFN-γ^+) cells ($CD4^+$ gated) and Tregs ($CD4^+$, $Foxp3^+$) from the draining LN of the indicated mice treated with TRA-8 on day 60 were

analyzed by flow cytometry. Data are presented as the mean ± s.e.m. * $P < 0.05$ and ** $P < 0.01$ between the indicated comparisons.

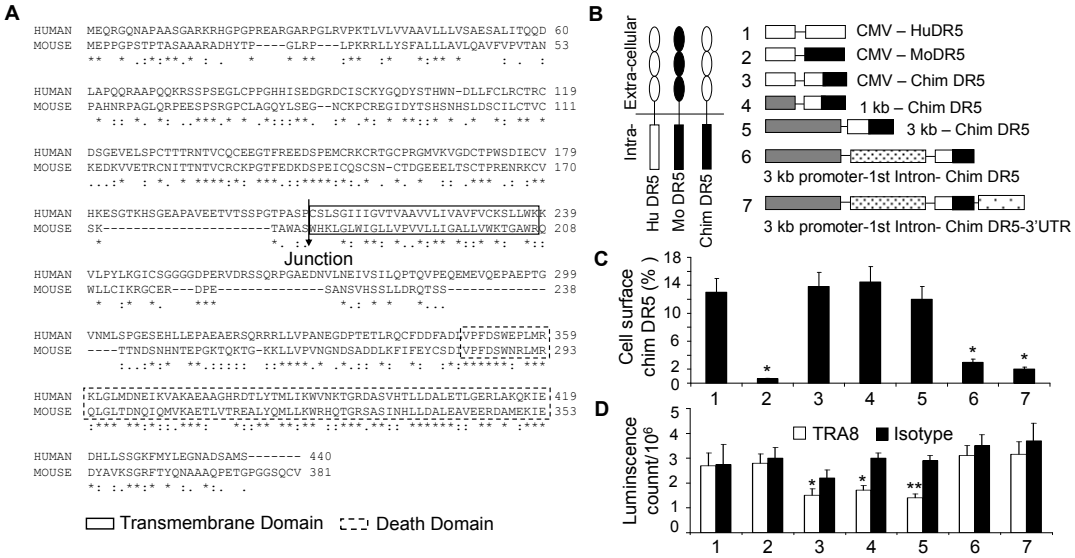

Figure 1. Human, mouse and chimeric DR5 and their expression and function in inducing apoptosis by TRA-8. **A,** Amino acid alignment of human and mouse DR5. Junction between human and mouse DR5 in the chimeric molecule, transmembrane, and death domain are as indicated. **B,** Schematic diagram representing the human, mouse and chimeric DR5 (left), and human, mouse and chimeric DR5 constructs generated with different promoters and regulatory elements (right). **C,** FACS analysis of cell surface expression of DR5 recognized by an anti-human DR5 antibody in NIH3T3 cells transiently transfected with the indicated constructs. Percentage of the hu/mo $DR5^+$ cells was shown. $N \geq 3$. * $P < 0.05$ versus result from construct 1. **D,** TRA-8 mediated killing in NIH3T3 transiently transfected with the indicated constructs. Cell viability was determined using the ATPLite assay. For panels C and D**,** the data represent the mean ± s.e.m. (n ≥ 3). Hu, human; mo, mouse; chim, chimeric. * $P < 0.05$ and ** $P < 0.01$ versus isotype control.

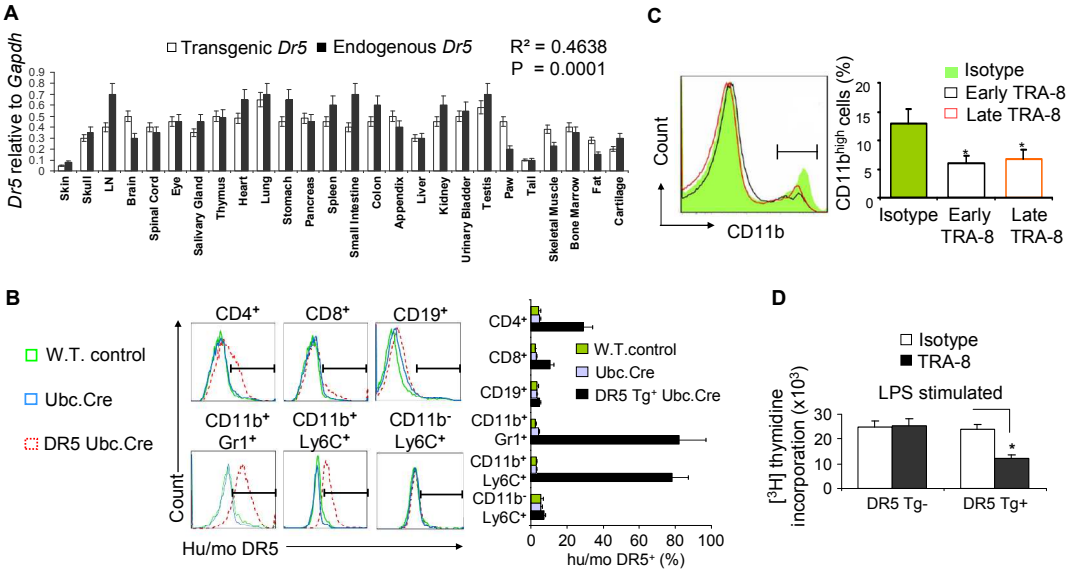

Figure 2. Hu/mo-chimeric Tg DR5 expression and function in Ubc.Cre DR5 Tg mice. **A,** Real-time PCR analysis of the chimeric *DR5* expression in the indicated tissues obtained from the Ubc.Cre DR5 double-positive transgenic mice after induction of Cre expression by tamoxifen. Expression is represented as the ratio of copy numbers of chimeric *Dr5* or endogenous mouse *Dr5* to those of *Gapdh*. The correlation R^2 and correlation *P* value are shown in the upper-right of the panel. **B,** Transgenic chimeric DR5 cell surface expression on different immune cells was analyzed by FACS (left panels). The chimeric DR5 expression is representative of three experiments (right panels). **C,** The percentage of $CD11b^{high}$ spleen macrophages from mice with and without TRA-8 treatment (0.2 mg, *i.v.*, twice/week for 2 months) was determined by FACS. Data represent the mean ± s.e.m. (n ≥ 3). **D,** Proliferation of LPS-stimulated spleen cells from DR5 Tg^- Ubc.Cre and hu/mo DR5 Tg^+ Ubc.Cre mice treated with TRA-8 or isotype control antibody was determined using the [^{3}H]-thymidine incorporation assay (n ≥ 3). * *P* < 0.05 versus isotype control.

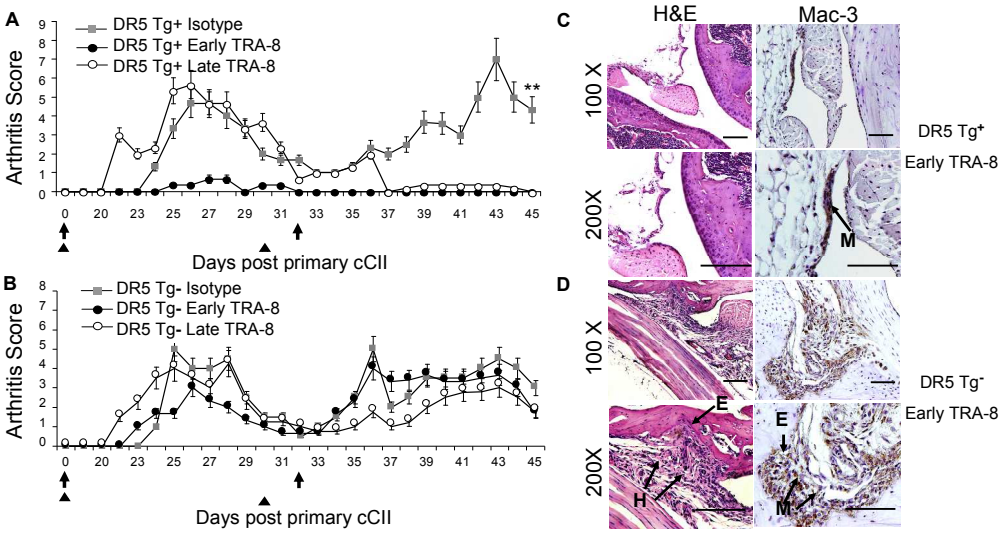

Figure 3. TRA-8 treatment prevents the development and attenuates the severity of CIA in hu/mo-chimeric DR5 Tg^+ Ubc.Cre mice. CIA was induced in the indicated DR5 Tg^+ (**A**) and DR5 Tg^- mice (**B**) as described in detail in the methods section. Chicken type II collagen emulsified in CFA and IFA was administered intradermally on day 0 and day 32 respectively (arrows). Early and late TRA-8 treatment (0.2 mg/mouse, once per week) was initiated on day 0 and day 30 respectively (arrow heads) and continued until sacrifice. Clinical scores (0-3 per paw; n=6 per group) were assessed daily until the mice were sacrificed. Data are presented as mean arthritis score ± s.e.m.. ** $P < 0.01$ versus TRA-8-treated groups at the same time point. **C** and **D,** Representative H&E and Mac-3 immunohistochemical staining of the knee joint sections from a TRA-8 treated hu/mo DR5 Tg^+ Ubc.Cre (**C**) or a TRA-8 treated DR5 Tg^- Ubc.Cre (**D**) mouse. The magnification of the objective lens used to acquire the indicated images is shown in the left. E, erosion; H, hyperplasia; M, macrophages, (Scale bar, 100 μm).

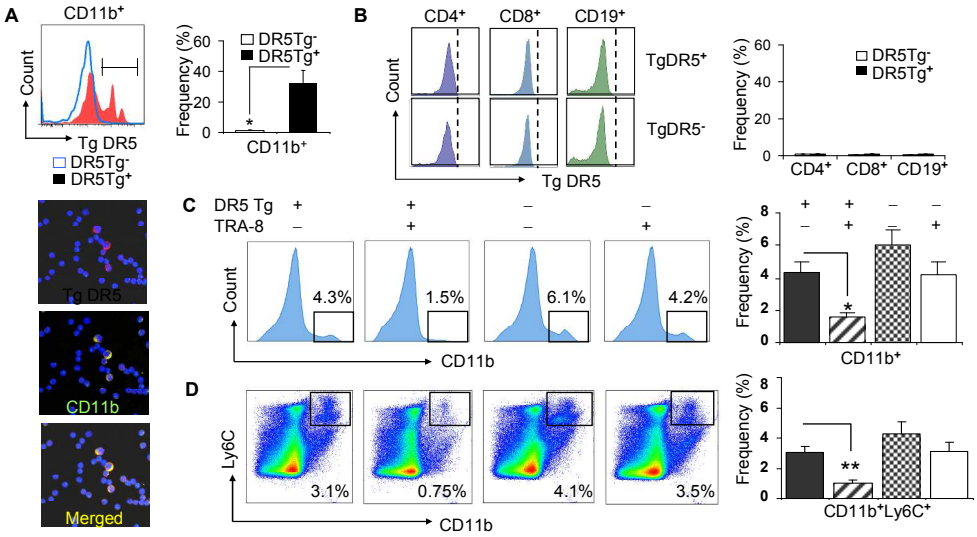

Figure 4. Expression of hu/mo-chimeric DR5 in macrophages and selective depletion by TRA-8 in hu/mo DR5 Tg^+ LysM.Cre mice with CIA. CIA was induced as described in the methods section. A group of mice were treated with TRA-8 (0.2 mg/mouse, *i.v.*, twice/week) until analysis at day 60 post primary cCII injection. **A,** Flow cytometry analysis of the expression of Tg DR5 as indicated by cell surface binding to an anti-human DR5 antibody on $CD11b^+$ cells from the draining LN (upper panels). Chimeric Tg DR5 expression on $CD11b^+$ cells by immunofluoresence staining of CD11b and hu/mo-chimeric DR5 on cells prepared by cytospin without cell permeabilization (lower panels). Chimeric Tg DR5 was detected using the Tyramide Signal Amplification (TSA) technique. **B,** Flow cytometry analysis of the expression of Tg DR5 by cell surface binding to an anti-human DR5 antibody on the indicated cell types from the draining LN. **C** and **D,** TRA-8 treatment depleted $CD11b^+$ macrophages and $CD11b^+Ly6C^+$ inflammatory macrophages from draining LN from the indicated groups of mice by dot plot (left) and bar graph (right) analysis. Data represent the mean ± s.e.m. (n ≥ 3). * $P < 0.05$ and ** $P < 0.01$ between the indicated comparisons.

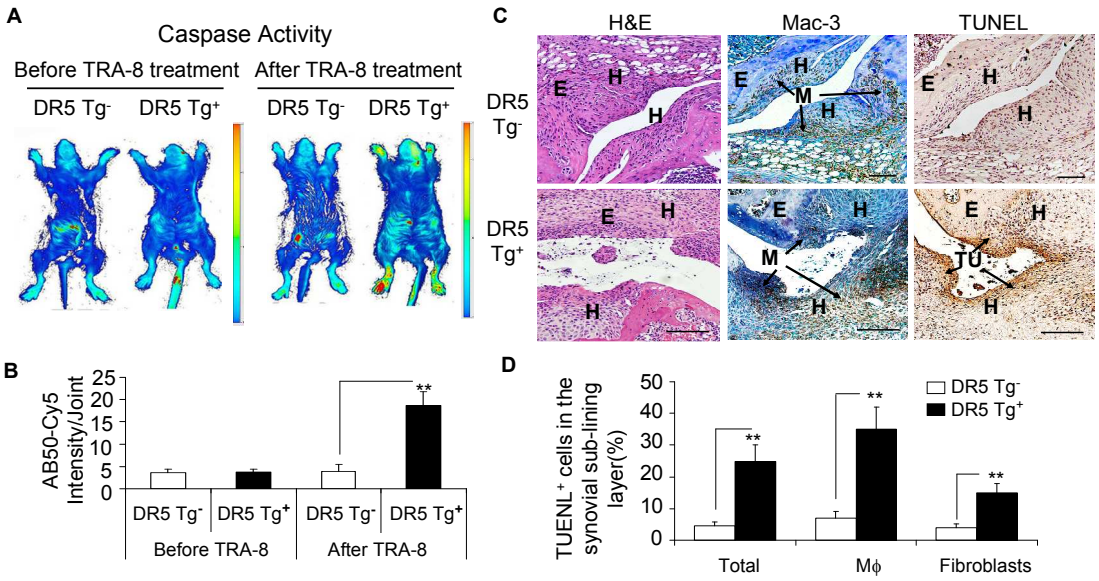

Figure 5. Apoptosis induced by TRA-8 in the joints of hu/mo-chimeric DR5 Tg$^+$ LysM. Cre mice with CIA. **A,** *In vivo* imaging of TRA-8 induced apoptosis in joints. **B,** Quantitation of the imagines. DR5 Tg$^+$ LysM.Cre and control LysM.Cre mice were induced to develop CIA. At 8 week after induction, baseline levels of the caspase activity were measured using the caspase-targeted activity based probe AB50-Cy5 (left panel). Mice were then treated with TRA-8 (0.2 mg, day 0 and 3) and apoptosis imaging using AB50-Cy5 was performed on the same mice on day 6 after initiating TRA-8 treatment (right panel). **C,** Immediately after the second AB50-Cy5 imaging, the joints were removed, fixed and processed for H.&E. (left), Mac-3 staining (middle, counterstained with methyl green), and TUNEL (right, counterstained with hematoxyline). **D,** Quantitative analysis of the TUNEL$^+$ cells of the indicated cell types in synovium. The values on the Y-axis represent the percentages of TUNEL-positive cells of the indicated cell types. Five randomly chosen fields of synovium were evaluated for each section. E, erosion; H, hyperplasia; M, macrophages, and TU, TUNEL. Scale bar, 100 μm. Data represent mean ± s.e.m. (n ≥ 3). ** $P < 0.01$ between the indicated comparisons.

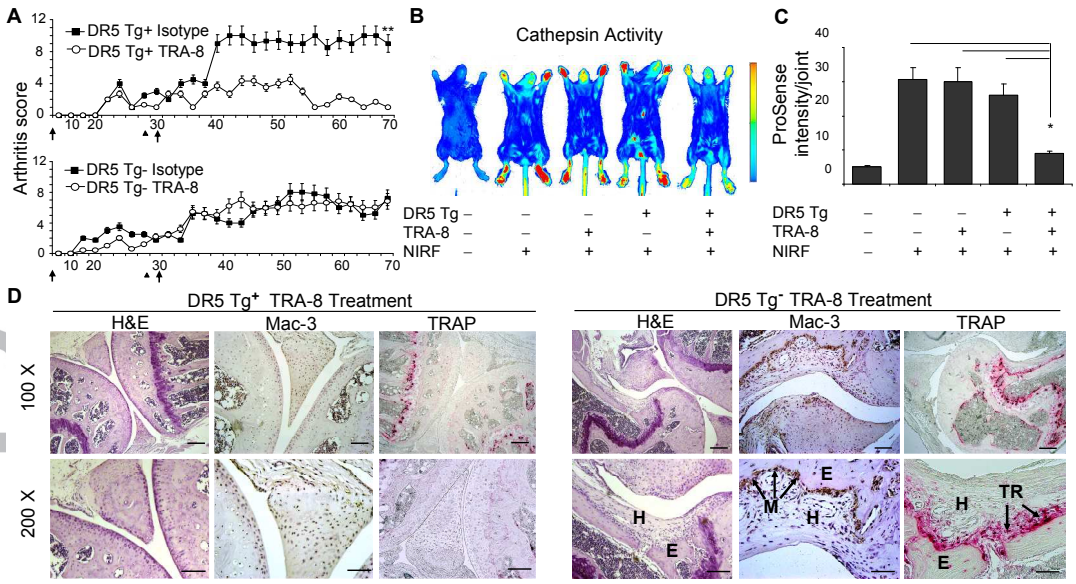

Figure 6. TRA-8 treatment ameliorates the severity of CIA in hu/mo-chimeric DR5 Tg^{+} LysM.Cre mice. **A,** CIA was induced in hu/mo DR5 Tg^{+} LysM.Cre (upper panel) and control DR5 Tg^{-} LysM.Cre mice (lower panel). Arrows indicate the intradermal injection of chicken type II collagen on day 0 and 30. TRA-8 treatment was initiated on day 28 (arrow heads). Clinical scores (n = 6 per group) were assessed until the mice were sacrificed on day 60. Data are presented as the mean clinical score ± s.e.m. * $P < 0.05$ and ** $P < 0.01$ versus TRA-8 treated group at the indicated time point. **B,** Cathepsin activity in joints was measured by *in vivo* imaging using the NIRF-probe ProSense 750. **C,** Quantitative analysis of ProSense 750 intensity. Data are presented as the mean ± s.e.m. * $P < 0.05$ between the indicated comparisons. **D,** Histological assessment of representative knee joints from TRA-8-treated DR5 Tg^{+} LysM.Cre DR5 (left panels) and DR5 Tg^{-} LysM.Cre mice (right panels), which included H&E , Mac-3, and TRAP staining as indicated (scale bar: 100 μm). Both groups were treated with TRA-8 weekly for one month. E, erosion; H, hyperplasia; M, macrophages, and TR, TRAP.

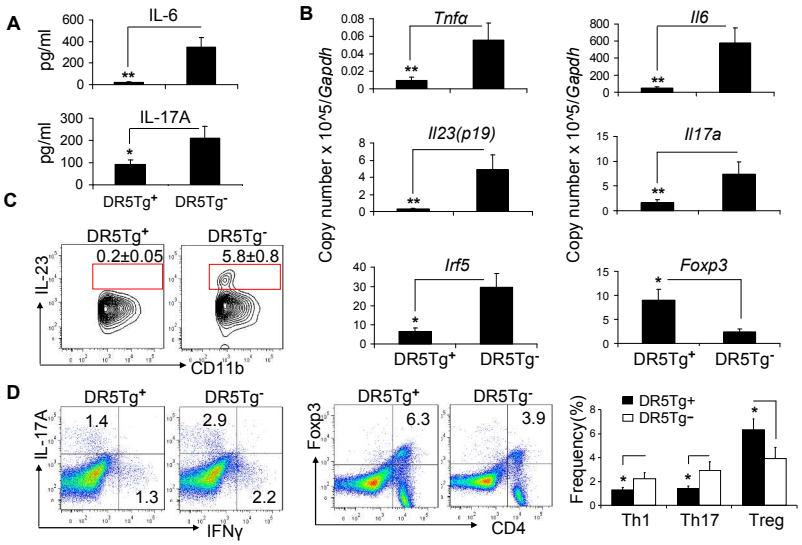

Figure 7. TRA-8 treatment decreases the expression of proinflammatory cytokines and exhibits immunomodulatory effects in hu/mo DR5 Tg^+ LysM.Cre mice. CIA was induced in hu/mo DR5 Tg^+ LysM.Cre and control DR5 Tg^- LysM.Cre mice as described in the methods section. TRA-8 treatment was initiated on day 28 until analysis at day 60 post primary cCII injection. **A,** Sera levels of IL-6 and IL-17A of indicated mice with TRA-8 treatment were analyzed by ELISA. **B,** Absolute copy numbers of *Tnfa, Il6, Il17, Il23(p19), Irf5* and *Foxp3* of synovium of the indicated mice were determined by qRT-PCR and represented as copy number $x10^5$/*Gapdh*. **C**, Percentage of IL-23^+ CD11b^+ macrophages from the draining LN of the indicated mice treated with TRA-8 on day 60 (CD11b^+ gated) was determined by flow cytometry. **D**, Percentage of Th17 (IL-17^+) and Th1 (IFN-γ^+) cells (CD4^+ gated) and Tregs (CD4^+, Foxp3^+) from the draining LN of the indicated mice treated with TRA-8 on day 60 were analyzed by flow cytometry. Data are presented as the mean ± s.e.m. * $P < 0.05$ and ** $P < 0.01$ between the indicated comparisons.